

Electrochemical study of Magnetite-CH composite carbon paste modified electrode

AL. Kavitha^{*,†} and Kumanan Bharathi Yazhini^{**}

^{*}Kings College of Engineering, Punalkulam 613303, India

^{**}Alagappa University, Research Scholar, Karaikudi, India

(Received 29 July 2015 • accepted 5 February 2016)

Abstract—Magnetite nanoparticles were synthesized by coprecipitation and characterized. The average particle size was 22-50 nm by XRD and AFM. Chitosan was prepared from crab shells and characterized. Magnetite-chitosan composite carbon paste modified electrode was prepared and characterized by using XRD, FT-IR and SEM technique. The electrochemical responses of this Magnetite-CH composite electrode were studied in potassium ferrocyanide/KCl system using cyclic voltammetry and electrochemical impedance spectroscopy. The cyclic voltammetric and EIS studies indicated better electron transfer of magnetite-CH composite (3:1) carbon paste modified electrodes compared to bare, magnetite, chitosan composite electrodes. The surface parameters like surface coverage (Γ), Diffusion coefficient (D_0), and rate constant (k_s) were studied. The shelf-life of the developed electrode system is about 12 weeks under refrigerated conditions.

Keywords: Magnetite, Chitosan, Nanocomposite, Carbon Paste, Modified Electrode

INTRODUCTION

Among the various nanomaterials, iron oxide nanoparticles have gained increased interest due to promising applications as drug delivery, hyperthermia treatment, cell separation, biosensors, enzymatic assays etc [1,2]. However, pure iron oxide nanoparticles themselves may not be very useful in practical applications because they are more likely to aggregate for their large ratio of surface area to volume and strong magnetic dipole-dipole attractions between particles compared with other nanoparticles [3], and have limited functional groups for selective binding. Among the various biopolymers, chitosan (CH) along with nanoparticles has been utilized as a stabilizing agent due to its excellent film-forming ability, mechanical strength, biocompatibility, non-toxicity, high permeability towards water, susceptibility to chemical modifications, cost-effectiveness etc. for enzyme (GOx) immobilization. Chitosan with iron oxide composites has attracted much attention since surface functionalization of the nanoparticles allows their covalent attachment, self assembly and organization on surface, making them promising for the loading of biomolecules in a favorable microenvironment for the development of a biosensor and biomedical applications [4-14].

Carbon paste electrodes (CPEs) belong to promising electrochemical or bioelectrochemical sensors of wide applicability. CPEs represent one of the most frequent types of working electrodes. The overwhelming number of CPEs used worldwide belongs to pastes with insulating liquids (paraffin oil, silicon oil, bromonaphthalene, tricresyl phosphate and others). The basic requirements for a pasting liquid are its practical insolubility in the solution under measurement, low vapor pressure to ensure both mechanical stability

and long life-time, its electrochemical inactivity in the potential window of interest [15,16]. A holder for carbon pastes can be realized as a well drilled into a short Teflon rod, a glass tube or a polyethylene syringe filled with a paste, which is electrically contacted through a conducting wire. Such constructions are very simple. Different carbon-based materials such as glassy carbon (GC), graphite, carbon paste (CP), carbon fibers, porous carbon and carbon spheres are commonly employed as electrode materials or as biosensor immobilization matrices [17-22].

In the present work, magnetite nanoparticles were synthesized and composited with prepared chitosan and added to carbon paste for the preparation of modified electrode system. XRD, FT-IR, SEM techniques were employed for the characterization. The electrochemical behavior of the composite electrode was thoroughly investigated by cyclic voltammetry and electrochemical impedance spectroscopy.

EXPERIMENTAL

1. Reagents

AR grade chemicals such as ferric chloride (FeCl_3), ferrous sulfate (FeSO_4), ammonia, Acetone ($\text{C}_3\text{H}_6\text{O}$), hydrochloric acid, sodium hydroxide, Acetic acid, Zinc chloride, graphite powder and paraffin oil were purchased from Merck. All these chemicals were used without further purification. TKA-high pure water was used to prepare solutions.

2. Characterization

The structure and particle size of magnetite nanoparticles were investigated by using X-ray diffraction (X'Pert PRO) instrument. FT-IR spectrophotometer (Shimadzu 8400) was used to characterize magnetite-chitosan nanocomposite. The surface morphological studies were investigated using a scanning electron microscope (Hitachi S3000H). The carbon paste electrode tip was cut into

[†]To whom correspondence should be addressed.

E-mail: alkavitha82@gmail.com

Copyright by The Korean Institute of Chemical Engineers.

1 cm² area and then characterized for SEM analysis. Cyclic voltammetric (CV) analysis was performed using a CH-620A instrument for electron transfer reaction and experiments were conducted with a three electrode system (carbon paste modified electrode as working electrode, Pt foil as counter electrode and Ag/AgCl as reference electrode). The electrochemical impedance spectroscopy (EIS) was recorded with AUTOLAB for electron transfer resistance (R_{CT}) measurements.

3. Preparation of Magnetite Nanoparticles

Magnetite nanoparticles were prepared by co-precipitation of Fe²⁺ and Fe³⁺ ions with ammonia. Ferric chloride and ferrous sulfate (mole ratio 2:1) were dissolved in water at a concentration of 0.3 M Fe ions by passing N₂ gas for five minutes. Chemical precipitation was achieved at 25 °C under vigorous stirring by adding 30 ml of ammonium hydroxide solution (29.6%). During the reaction process, the pH was maintained at about 10.5. Black precipitate of magnetite thus obtained was heated at 80 °C for 30 min and then subjected to washing with deionized water and ethanol several times. Finally, it was dried in a vacuum oven at 70 °C for about 3 hours.

4. Preparation of Chitosan

For the preparation of chitin, crab shells were collected from the Nagapattinam coastal area. The shells were washed well with sea water and again with fresh water and then powdered by crushing in a mortar. About 50 g of powdered shell was taken in a 500 ml beaker. 250 ml of 5% HCl was added to remove calcium carbonate present in the shell. The mixture was allowed to stand for about 2 hours. It was then filtered with a muslin cloth and the residue was transferred into a 500 ml beaker. 250 ml of 5% NaOH was added to it slowly to remove protein present in the shell. The mixture was then allowed to stand for about 3 hours and filtered through muslin cloth to get chitin. 2 g of this chitin was added to 60% anhydrous ZnCl₂ and heated in a boiling water bath for 30 minutes. The mixture was dissolved in dilute acetic acid. It was then filtered to remove the unreacted chitin and other impurities. Chitosan was precipitated from the filtrate using 20% NaOH solution, filtered and then air dried.

5. Preparation of Magnetite-chitosan (3:1) Composite Containing Carbon Paste Electrode

The carbon paste electrode (CPE) was prepared in a regular way

by mechanically mixing graphite powder and paraffin oil in an agate mortar for 30 min. CPE containing chitosan (0.1 g)-magnetite (0.3 g) nanocomposite (1:3) was prepared in the similar procedure (initially, the CH solution was prepared by dissolving CH in acetate buffer (0.05 M, pH 4.2) solution, a calculated amount of magnetite nanoparticles was dispersed in the CH solution by stirring at room temperature, and finally, a highly viscous solution of CH with uniformly dispersed magnetite nanoparticle was obtained). Then magnetite-chitosan composite and paraffin oil were mixed for 1 min, followed by the incorporation of the graphite powder and mixing continued for additional 30 min. A portion of the paste obtained was packed firmly into a glass tube. Electrical contact was established through a copper wire. The electrode surface was smoothed on a weighing paper before starting every new experiment.

RESULTS AND DISCUSSION

1. Characterization of Magnetite Nanoparticles, Chitosan and Magnetite-chitosan Composite Carbon Paste Modified Electrode

Formation of magnetite nanoparticles and chitosan was confirmed by XRD pattern [23,24] and shown in Fig. 1. The average particle size was calculated with Scherrer formula and found to be 52 nm. FT-IR spectrum of magnetite nanoparticles exhibited peak in the frequency region 586 cm⁻¹. The peak at about 3,400 cm⁻¹ is attributed to the presence of -OH group. FT-IR spectrum of chitosan shows a band of 1,596 cm⁻¹ for N-H bending vibration and a peak of 1,384 cm⁻¹ for C-O stretching of primary alcoholic group [25].

The bare and modified carbon paste electrode surfaces were characterized by XRD, FT-IR and SEM techniques. Fig. 2 depicts the XRD patterns of bare electrode, modified electrode of chitosan, magnetite and magnetite-chitosan composite. The magnetite and chitosan were present in the modified carbon matrix. This is evinced by comparing the XRD pattern obtained for the composite with the standard JCPDS 89-6466 data for magnetite and the standard JCPDS 008-0415 data for carbon.

The FT-IR spectrum of carbon paste electrode containing magnetite nanoparticles confirmed the presence of magnetite with a peak at 586 cm⁻¹ (Fig. 3(a)). The FT-IR spectrum of carbon paste

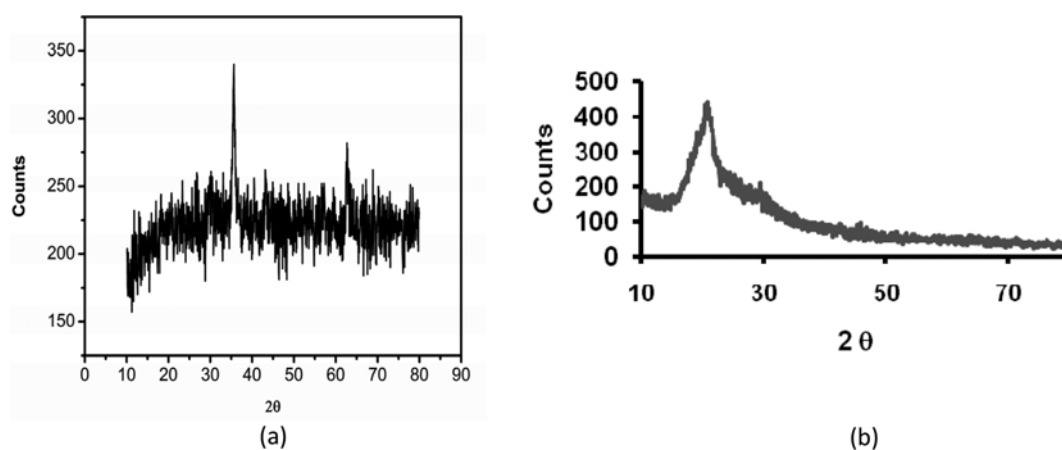


Fig. 1. XRD of (a) magnetite nanoparticles, (b) chitosan.

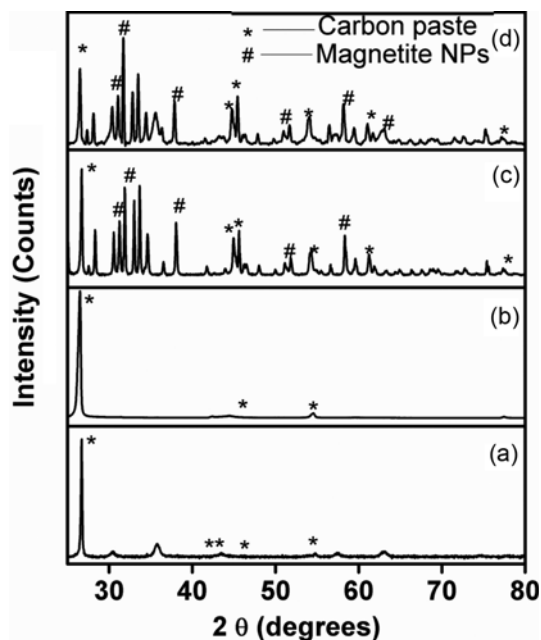


Fig. 2. XRD of bare carbon paste electrode (a) and the electrode containing chitosan (b), magnetite nanoparticles (c), magnetite-CH composite (d).

electrode containing chitosan (Fig. 3(b)) displayed bands at 3,200–3,400 cm^{-1} due to the stretching mode of -OH and -NH₂ groups, peak at 1,746 cm^{-1} for C-O stretching (C=O in carboxylic acid), peak at 1,650 cm^{-1} for amide group (C-O stretching along with N-H deformation mode), peak at 1,625 cm^{-1} represents the C=C stretching mode and peak at 1,560 cm^{-1} for NH₂ group due to N-H deformation [26–34]. The FT-IR spectrum of carbon paste electrode containing magnetite-chitosan composite (Fig. 3(c)) exhibited characteristic bands of the functional group corresponding to pure CH and the magnetite nanoparticles. The bands corresponding to the -NH and -OH stretching modes were shifted to lower wavenumber in the spectrum of the magnetite-chitosan composite. This indicates that amine group of CH is involved in the assembling of magnetite nanoparticles.

Surface morphological studies of magnetite, chitosan, magnetite-chitosan and magnetite-chitosan-GOX bioelectrode were investigated by SEM analysis (Fig. 4). The images (a)–(c) clearly reveal

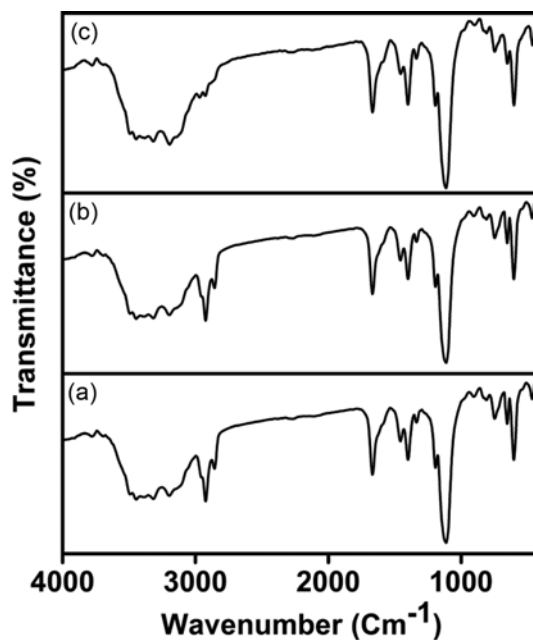


Fig. 3. FT-IR spectra of carbon paste electrode containing (a) magnetite, (b) chitosan, (c) magnetite-CH composite.

the changes in the morphology of the respective material content. The image c of composite shows that magnetite nanoparticles are uniformly embedded in the chitosan network.

2. Electrochemical Response Studies of Magnetite, Chitosan, Magnetite-CH, Composite Carbon Paste Modified Electrode

2-1. Cyclic Voltammetry

The initial concentration of CH (0.1 g) and magnetite nanoparticles (0.3 g) was made to prepare composite carbon paste electrode system. Voltammetric analysis was carried out in potassium ferrocyanide (2.5 mM)+KCl (0.1 M) at 1 : 1 ratio solution at 50 mV/s. The cyclic voltammograms of carbon paste electrode containing blank, magnetite, chitosan, magnetite-chitosan, in potassium ferrocyanide (2.5 mM)+KCl (0.1 M) at 1 : 1 ratio are shown in Fig. 5(a)–(d). In the presence of either blank or magnetite or chitosan or magnetite-chitosan composite on the electrode surface, redox peak was observed; the potential shifted to 0.21 V in magnetite-chitosan composite compared to individual composite. In the presence of magnetite nanoparticles incorporated into the CH matrix on the

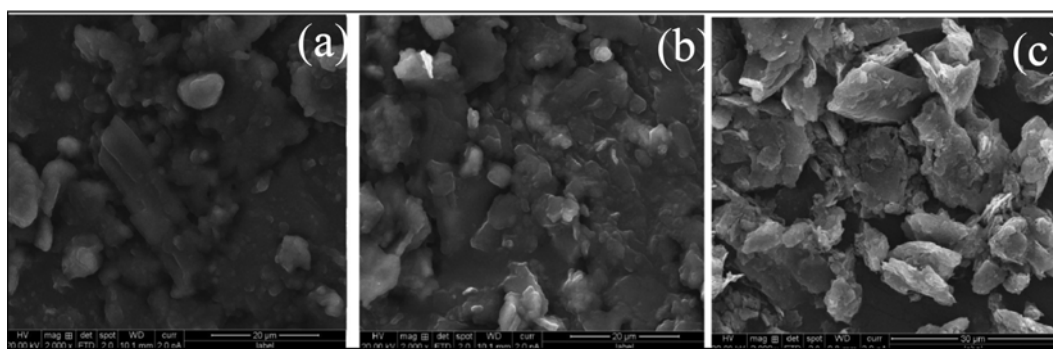


Fig. 4. SEM images of carbon paste electrode containing (a) magnetite, (b) chitosan, (c) magnetite-CH composite.

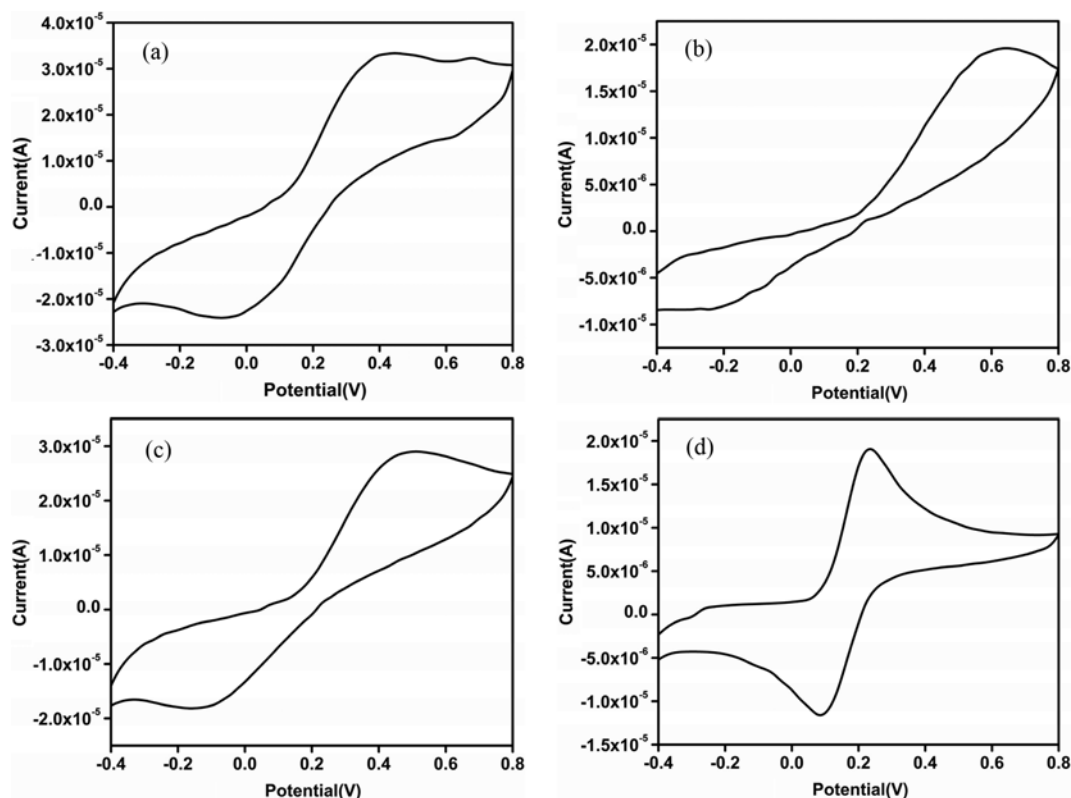


Fig. 5. (a) Cyclic voltammograms of blank carbon paste electrode containing at 50 mV/s scan rate in Potassium ferrocyanide (2.5 mM)+KCl (0.1 M)(1 : 1) ratio solution. (b) Cyclic voltammograms of Magnetite carbon paste electrode containing at 50 mV/s scan rate in Potassium ferrocyanide (2.5 mM)+KCl(0.1 M)(1 : 1) ratio solution. (c) Cyclic voltammograms of Chitosan carbon paste electrode containing at 50 mV/s scan rate in Potassium ferrocyanide (2.5 mM)+KCl(0.1 M)(1 : 1) ratio solution. (d) Cyclic voltammograms of Magnetite-Chitosan carbon paste electrode containing at 50 mV/s scan rate in Potassium ferrocyanide (2.5 mM)+KCl(0.1 M)(1 : 1) ratio solution.

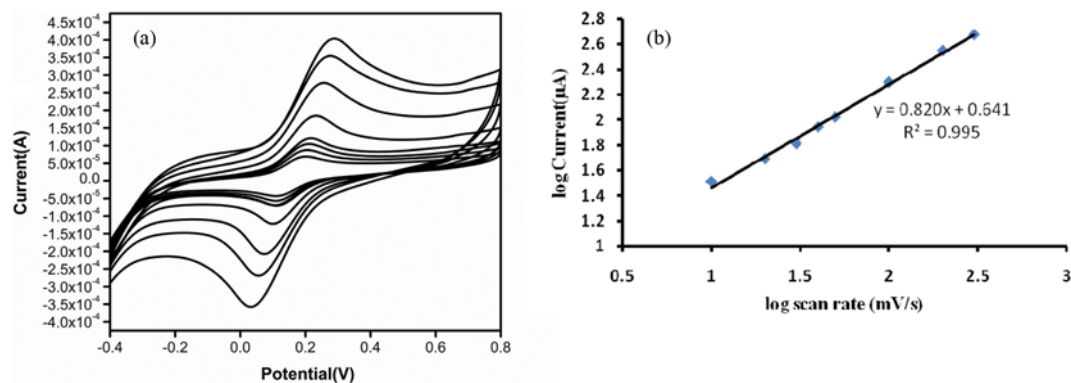


Fig. 6. (a) Cyclic voltammograms of Magnetite-Chitosan carbon paste electrode containing various scan rate (10, 20, 30, 40, 50, 100, 200 & 300 mV/s) in Potassium ferrocyanide (2.5 mM)+KCl(0.1 M)(1 : 1) ratio solution. (b) The plot of i_p (μ A) Vs ν (mV/s) in Potassium ferrocyanide (2.5 mM)+KCl(0.1 M)(1 : 1) ratio solution. Variation of the peak current with scan rate.

electrode surface, a better redox peak was obtained. This may be due to the interaction of magnetite nanoparticles with chitosan that resulted in increased electron mobility at the electrode surface. The reproducibility of this modified electrode was studied and found to be satisfactory.

A voltammetric study was carried out with magnetite-CH carbon paste electrode as a function of scan rate varying from 10 to 300 mV/s (Fig. 6(a)). The variation of the peak current with scan

rate is shown in (Fig. 6(b)). The peak current increased directly with the scan rate (with linear regression coefficient 0.994), indicating improved electrocatalytic behavior. The slope value obtained from $\log i_p$ against $\log \nu$ plot is above 0.5. Thus the redox reaction is considered as adsorption controlled process.

2-2. Electrochemical Impedance Spectroscopy

Electrochemical impedance spectroscopy studies (EIS) of bare carbon paste, magnetite, chitosan, magnetite-CH in carbon paste

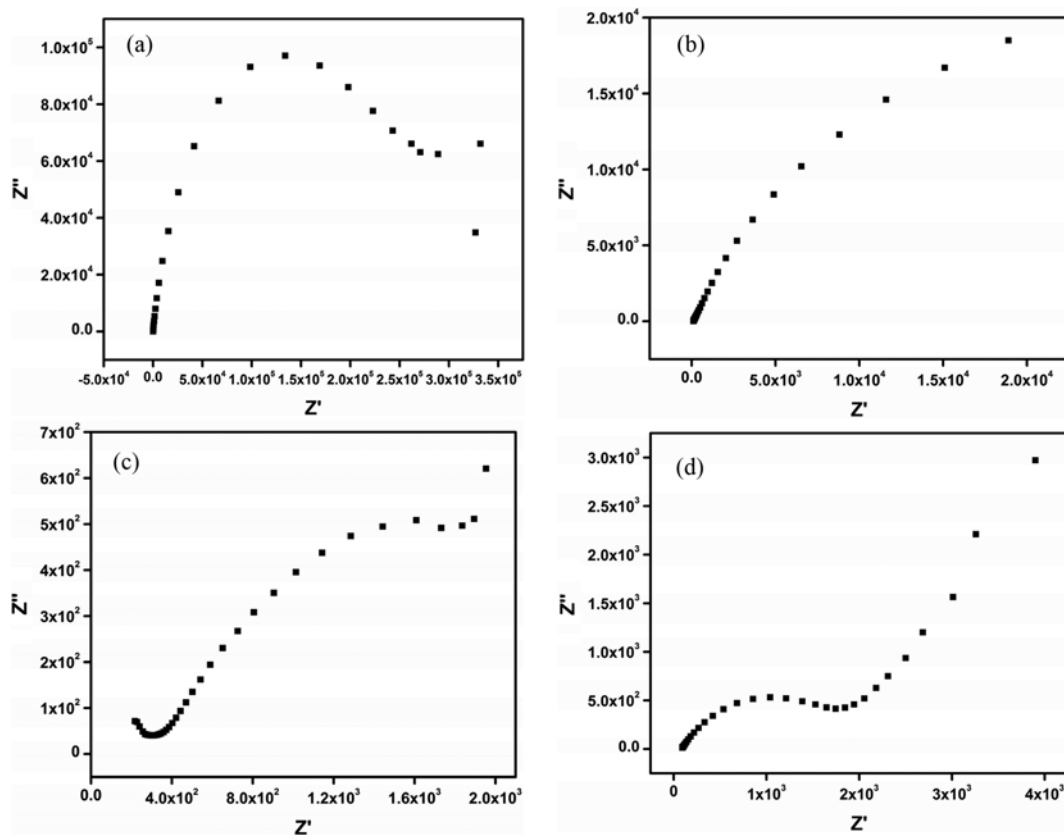


Fig. 7. (a) Electrochemical impedance spectra of Bare carbon paste electrode. (b) Electrochemical impedance spectra of carbon paste electrode containing magnetite. (c) Electrochemical impedance spectra of carbon paste electrode containing chitosan. (d) Electrochemical impedance spectra of carbon paste electrode containing magnetite-CH composite.

electrodes were investigated in potassium ferrocyanide (2.5 mM)/KCl (0.1 M) at 1 : 1 ratio in the frequency range 0.01-10⁵ Hz. In the EIS, the semicircle part corresponds to the electron transfer limited process; its diameter is equal to the electron transfer resistance, R_{CT} , which controls the electron transfer kinetics of the redox probe at the electrode interface. Fig. 7(a)-(d) presents the Nyquist plots of the impedance spectroscopy of the bare, magnetite, chitosan, magnetite-CH in carbon paste, respectively. Only a depressed semicircle is observed for bare CPE, indicating a rather slow electron-transfer rate between the couple of potassium ferrocyanide (2.5 mM)\KCl(0.1 M)(1 : 1) and the electrode surface. However, the

Nyquist plot of potassium ferrocyanide (2.5 mM)/KCl(0.1 M)(1 : 1) on the magnetite, chitosan CPE was quite different, which is formed of a semicircle followed by a straight line at high frequency range. The magnetite-CH composite greatly enhanced the electron-transfer rate of potassium ferrocyanide (2.5 mM)\KCl(0.1 M)(1 : 1) and the conductivity of the modified electrode. The results are similar to the electrochemical behavior of potassium ferrocyanide (2.5 mM)\KCl(0.1 M)(1 : 1) by CVs.

2-3. Surface Parameter Study of Magnetite-CH in Carbon Paste Electrode

The surface parameters like surface coverage (τ), Diffusion coef-

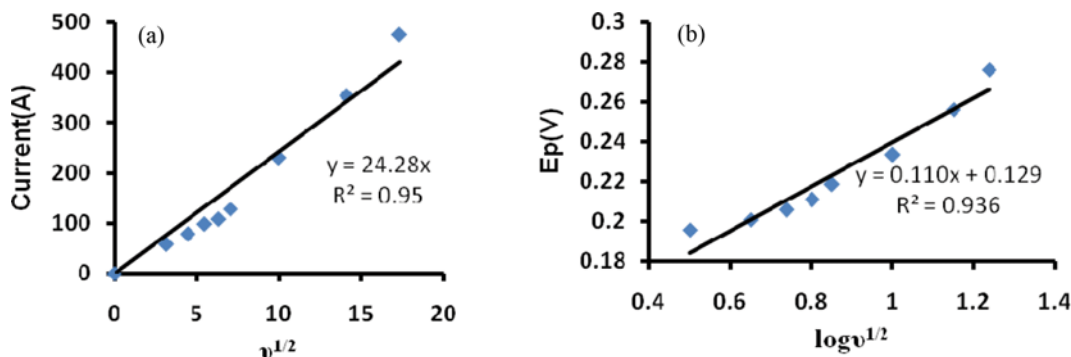


Fig. 8. The plot of (a) $i_p(\mu A)$ Vs $v^{1/2}(mv)$, (b) $E_p (V)$ Vs $\log v^{1/2}$.

efficient (D_0), and rate constant for electron transfer process using magnetite-CH carbon paste modified electrode were studied extensively. The surface coverage was calculated using the formula [35] is $0.8450 \times 10^{-5} \text{ mol}^{-1} \text{ cm}^{-2}$, since the area of the electrode is 0.196 cm^2 . The plot of i_p against $v^{1/2}$ ($i_p = 24.28 v^{1/2}$, $r^2 = 0.95$) gives the value of D_0 as $2.356 \times 10^{-1} \text{ cm}^2 \text{ s}^{-1}$ (Fig. 8(a)). The rate constant for the electron transfer process was calculated using E_p against $\log v^{1/2}$ plot (Fig. 8(b)) ($E_p = 0.110 \log v^{1/2} + 0.129$, $r^2 = 0.936$) and the value arrived at was $k_s = 2.3 \text{ s}^{-1}$. These results suggest that magnetite-CH in carbon paste electrode provides fast electron transfer between the redox center of the surface of electrode.

CONCLUSION

Magnetite-CH composite carbon paste modified electrodes were prepared and characterized. The electrochemical responses of this electrode have been studied in potassium ferrocyanide/KCl system using cyclic voltammetry and electrochemical impedance spectroscopy. The results of cyclic voltammetric and EIS studies indicated better electron transfer of magnetite-CH composite (3:1) carbon paste modified electrodes compared to bare, magnetite, chitosan composite electrodes. This type of electrode can be used for binding studies and biomedical applications.

REFERENCES

1. L. M. Rossi, A. D. Quach and Z. Rosenzweig, *Anal. Bioanal. Chem.*, **380**, 606 (2004).
2. A. K. Gupta and M. Gupta, *Biomaterials*, **26**, 3995 (2005).
3. G. Zhao, J. J. Feng, Q. L. Zhang, S. P. Li and H. Y. Chen, *Chem. Mater.*, **17**, 3154 (2005).
4. J. Singh, M. Srivastava, J. Duttac and P. K. Duttaa, *Int. J. Biol. Macromol.*, **48**, 170 (2011).
5. P. Chenliang, H. Bing, L. Wei, S. Yi, Y. Hong and Z. Xiaoxiong, *J. Mol. Catal. B: Enzym.*, **61**, 208 (2009).
6. L. Alejandro, C. Opez, B. Carola, L. Victoria, D. Calero and R. Carlos, *J. Mater. Chem.*, **19**, 6870 (2009).
7. N. Zheng, X. Zhou, W. Yang, X. Li and Z. Yuan, *Talanta*, **79**, 780 (2009).
8. Y. Wu, Y. Wang, G. Luo and Y. Dai, *Bioresour. Technol.*, **100**, 3459 (2009).
9. S. Wang, Y. Tan, D. Zhao and G. Liu, *Biosens. Bioelectron.*, **23**, 1781 (2008).
10. K. Donadel, D. V. F. Marcos, T. F. Valfredo, R. Mauricio, J. B. Nelson and C. M. Mauro, *Mater. Sci. Eng., C*, **28**, 509 (2008).
11. A. Kaushik, P. R. Solanki, A. A. Ansari, G. Sumana, S. Ahmad and B. D. Malhotra, *Sens. Actuat., B*, **138**, 572 (2009).
12. S. J. Cheong, C. M. Leea, S. L. Kim, H. J. Jeonga and E. M. Kim, *Int. J. Pharm.*, **372**, 169 (2009).
13. A. Kaushik, P. R. Solanki, A. A. Ansari, S. Ahmad and B. D. Malhotra, *Electrochem. Commun.*, **10**, 1364 (2008).
14. R. Singh, R. Verma, A. Kaushik, G. Sumana, S. Sood, R. K. Gupta and B. D. Malhotra, *Biosens. Bioelectron.*, **26**, 2967 (2011).
15. V. Karel, S. Ivan and M. Radovan, *J. Ser. Chem. Soc.*, **74**, 1021 (2009).
16. F. N. Comba, D. R. Maria, C. Lourdes, G. Silvia, H. Pilar and A. R. Gustavo, *Electroanalysis*, **22**, 1566 (2010).
17. R. N. Adams and M. Dekker, *Electrochemistry at Solid Electrodes*, Dekker, New York, **9**, 280 (1969).
18. T. Z. Peng, H. P. Li and S. W. Wang, *Analyst*, **118**, 1321 (1993).
19. J. H. Pei, Q. Jin and J. Y. Zhong, *Talanta*, **38**, 1185 (1991).
20. M. Albareda-Sirvent, A. Merkoci and S. Alegret, *Sens. Actuat. B*, **69**, 153 (2000).
21. N. Wisniewski and M. Reichert, *Colloids Surf., B: Biointerfaces*, **18**, 197 (2000).
22. S. Sotriropoulou, V. Gavalas, V. Vamvakaki and N. A. Chaniotakis, *Biosens. Bioelectron.*, **18**, 211 (2003).
23. J. Lai, K. V. P. M. Shafi, A. Ulman, K. Loos, N. Yang, M. H. Cui, T. Vogt, C. Estournes and D. C. Locke, *J. Am. Chem. Soc.*, **125**, 11470 (2004).
24. Z. Li, L. Yubao, Y. Aiping, P. Xuelin, W. Xuejiang and Z. Xiang, *J. Mater. Sci. Mater. Med.*, **16**, 213 (2005).
25. Y. Z. Lian, J. Z. Xin, W. S. Han, R. C. Gui, X. X. Jun and L. S. Yong, *Curr. Appl. Phys.*, **10**, 828 (2010).
26. Y. Wei, X. Ling, L. Zou, D. Lai, H. Lu and Y. Xu, *Colloids Surf., A: Physicochem. Eng. Aspects*, **482**, 507 (2015).
27. F. Alimohammadi, M. Parvinzadeh Gashti, A. Shamei and A. Kiumarsi, *Superlattices, Microstruct.*, **52**, 50 (2012).
28. F. Alimohammadi, M. Parvinzadeh Gashti and A. Shamei, *Prog. Org. Coat.*, **74**, 470 (2012).
29. M. Parvinzadeh Gashti and A. Almasian, *Composites: Part B*, **45**, 282 (2013).
30. K. Deng, C. Li, X. Qiu, J. Zhou and Z. Hou, *J. Electroanal. Chem.*, **755**, 197 (2015).
31. M. Parvinzadeh Gashti, M. Ourquin, M. Stir and J. Hulliger, *J. Mater. Chem.*, **1**, 1501 (2013).
32. M. Ibrahim, O. Osman and A. Aziz Mahmoud, *J. Omput. Theor. Nanos*, **8**, 117 (2011).
33. M. Parvinzadeh Gashti, M. Burgener, M. Stir and J. Hulliger, *J. Colloid Interface Sci.*, **431**, 49 (2014).
34. A. Pawlak and M. Mucha, *Thermochim. Acta*, **396**, 153 (2013).
35. P. R. Solanki, S. K. Arya, S. P. Singh, M. K. Pandey and B. D. Malhotra, *Sens. Actuat. B*, **123**, 829 (2007).